Zwicky Transient Facility Constraints on the Optical Emission from the Nearby Repeating FRB 180916.J0158+65

Igor Andreoni[1] ![ORCID], Wenbin Lu[1] ![ORCID], Roger M. Smith[2], Frank J. Masci[3] ![ORCID], Eric C. Bellm[4] ![ORCID], Matthew J. Graham[1] ![ORCID], David L. Kaplan[5] ![ORCID], Mansi M. Kasliwal[1] ![ORCID], Stephen Kaye[2], Thomas Kupfer[6] ![ORCID], Russ R. Laher[3] ![ORCID], Ashish A. Mahabal[1] ![ORCID], Jakob Nordin[7], Michael Porter[2], Thomas A. Prince[1] ![ORCID], Dan Reiley[2], Reed Riddle[2] ![ORCID], Joannes Van Roestel[1] ![ORCID], and Yuhan Yao[1] ![ORCID]

[1] Division of Physics, Mathematics and Astronomy, California Institute of Technology, Pasadena, CA 91125, USA; andreoni@caltech.edu
[2] Caltech Optical Observatories, California Institute of Technology, Pasadena, CA 91125, USA
[3] IPAC, California Institute of Technology, 1200 E. California Boulevard, Pasadena, CA 91125, USA
[4] DIRAC Institute, Department of Astronomy, University of Washington, 3910 15th Avenue NE, Seattle, WA 98195, USA
[5] Center for Gravitation, Cosmology, and Astrophysics, Department of Physics, University of Wisconsin–Milwaukee, P.O. Box 413, Milwaukee, WI 53201, USA
[6] Kavli Institute for Theoretical Physics, University of California, Santa Barbara, CA 93106, USA
[7] Institute of Physics, Humboldt-Universität zu Berlin, Newtonstr. 15, D-12489 Berlin, Germany

Received 2020 May 14; revised 2020 May 16; accepted 2020 May 17; published 2020 June 5

Abstract

The discovery rate of fast radio bursts (FRBs) is increasing dramatically thanks to new radio facilities. Meanwhile, wide-field instruments such as the 47 deg^2 Zwicky Transient Facility (ZTF) survey the optical sky to study transient and variable sources. We present serendipitous ZTF observations of the Canadian Hydrogen Intensity Mapping Experiment (CHIME) repeating source FRB 180916.J0158+65 that was localized to a spiral galaxy 149 Mpc away and is the first FRB suggesting periodic modulation in its activity. While 147 ZTF exposures corresponded to expected high-activity periods of this FRB, no single ZTF exposure was at the same time as a CHIME detection. No $>3\sigma$ optical source was found at the FRB location in 683 ZTF exposures, totaling 5.69 hr of integration time. We combined ZTF upper limits and expected repetitions from FRB 180916.J0158+65 in a statistical framework using a Weibull distribution, agnostic of periodic modulation priors. The analysis yielded a constraint on the ratio between the optical and radio fluences of $\eta \lesssim 200$, corresponding to an optical energy $E_{\rm opt} \lesssim 3 \times 10^{46}$ erg for a fiducial 10 Jy ms FRB (90% confidence). A deeper (but less statistically robust) constraint of $\eta \lesssim 3$ can be placed assuming a rate of $r(>5\,{\rm Jy\,ms}) = 1\,{\rm hr}^{-1}$ and 1.2 ± 1.1 FRB occurring during exposures taken in high-activity windows. The constraint can be improved with shorter per-image exposures and longer integration time, or observing FRBs at higher Galactic latitudes. This work demonstrated how current surveys can statistically constrain multiwavelength counterparts to FRBs even without deliberately scheduled simultaneous radio observation.

Unified Astronomy Thesaurus concepts: Neutron stars (1108); Transient sources (1851); Optical bursts (1164); Radio bursts (1339); Compact objects (288)

Supporting material: data behind figure

1. Introduction

Fast radio bursts (FRBs) are cosmological millisecond-duration radio flashes that are now discovered routinely by facilities such as the Parkes telescope (e.g., Bhandari et al. 2018), the Canadian Hydrogen Intensity Mapping Experiment (CHIME; CHIME/FRB Collaboration et al. 2018), the updated Molonglo Observatory Synthesis Telescope (UTMOST; e.g., Farah et al. 2018), the Australian Square Kilometre Array Pathfinder (e.g., Shannon et al. 2018), and the Deep Synoptic Array (DSA; Kocz et al. 2019; Ravi et al. 2019). Several FRBs were found to repeat (Spitler et al. 2016; Kumar et al. 2019; CHIME/FRB Collaboration et al. 2019a, 2019b; Fonseca et al. 2020), which suggests that a fraction (if not all; see Ravi 2019) of FRB progenitors are not disrupted by the outburst.

Searches for optical or high-energy counterparts were conducted during standard "triggered" follow-up observations (e.g., Petroff et al. 2015; Shannon & Ravi 2017; Bhandari et al. 2018) as well as during simultaneous observations with wide-field telescopes (e.g., DeLaunay et al. 2016; Martone et al. 2019; Tingay & Yang 2019) or targeting repeating FRBs (e.g., Scholz et al. 2016, 2017; Hardy et al. 2017; MAGIC Collaboration et al. 2018). A marginal gamma-ray candidate was found by DeLaunay et al. (2016) possibly associated with FRB 131104, but a robust transient counterpart to an FRB is yet to be discovered. The recent detection of a bright >1.5 MJy ms radio burst probably associated with the Galactic soft gamma-ray repeater SGR 1935+2154 (Bochenek et al. 2020) may offer an important piece to solve the FRB puzzle.

A particularly interesting repeating source was discovered with CHIME FRB 180916.J0158+65 (CHIME/FRB Collaboration et al. 2019b) and its monitoring showed the first evidence for a periodicity in its activity rate of 16.35 ± 0.18 day (The CHIME/FRB Collaboration et al. 2020). The source was precisely localized to a nearby massive spiral galaxy at a luminosity distance of 149 ± 0.9 Mpc (Marcote et al. 2020), which presents an opportunity to study its host in detail and to search for possible transient/variable counterparts. Multiwavelength follow-up observations of FRB 180916.J0158+65 were recently performed in the radio, optical, X-ray, and gamma-ray bands (Casentini et al. 2020; Panessa et al. 2020; Pilia et al. 2020; Scholz et al. 2020; Tavani et al. 2020; Zampieri et al. 2020). However, no transient or variable counterpart to this source has been detected outside radio bands.
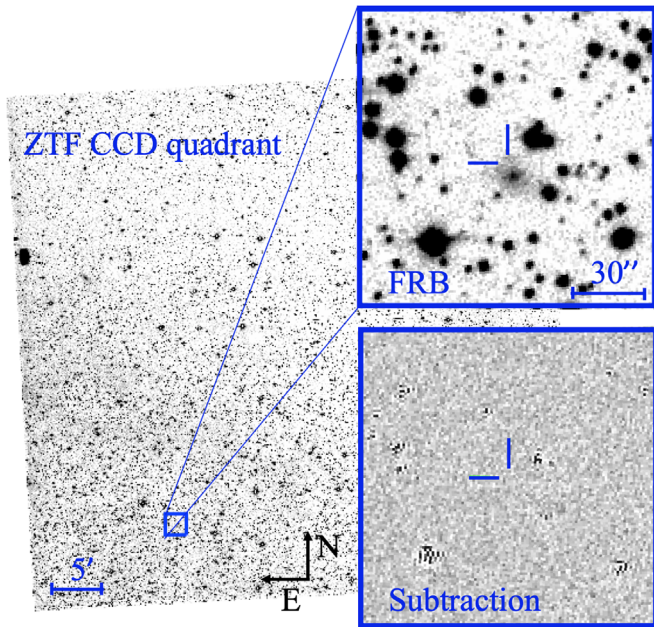
Figure 1. The location of FRB 180916.J0158+65 was observed during the ZTF survey of the northern sky. The image shows a template image of the ZTF 3k × 3k pixel CCD quadrant (1 out of 64 CCD quadrants that cover 47 deg^2 in total per exposure) including the FRB host galaxy. The top panel offers a closer view of the FRB location, and the lower panel shows the result of image subtraction.

The Zwicky Transient Facility (ZTF; Bellm et al. 2019; Graham et al. 2019; Masci et al. 2019) on the optical Samuel Oschin 48 inch Telescope at Palomar Observatory observed the coordinates of FRB 180916.J0158+65 serendipitously during its first 2 yr of activity (Figure 1). As a result of our analysis, no variable optical counterpart to FRB 180916.J0158+65 was found in ZTF data. We describe the observations in Section 2 and the statistical method to constrain the optical-to-radio fluence ratio in Section 3. The results are presented in Section 4. We compare our constraints to previous works in Section 5, and a summary with future prospects is provided in Section 6.

2. Data Analysis

ZTF surveys the sky with a typical exposure time of 30 s per image. A total of 683 science images were used in this work that include the coordinates of FRB 180916.J0158+65 (R.A. J2000 = 01:58:00.750, decl. J2000 = 65:43:00.315; Marcote et al. 2020), for a total exposure time of 5.69 hr (Table 1). The images were acquired from 2018 May 31 to 2019 December 22[8] during the ZTF public survey as well as part of the ZTF partnership and Caltech surveys (PI: Kulkarni, PI: Prince, PI: Graham). Figure 2 shows the temporal distribution of ZTF observations and CHIME detections of FRB 180916.J0158+65 (Marcote et al. 2020; The CHIME/FRB Collaboration et al. 2020). Assuming a periodic modulation of 16.35 days and 2 × 2.6 day time windows centered on activity peaks that include all the FRBs published in The CHIME/FRB Collaboration et al. (2020), 147 ZTF images were acquired during high-activity times of FRB 180916.J0158+65, marked with purple stripes in Figure 2. The closest ZTF exposure to an

FRB detection was acquired 11.76 minutes before the FRB found on 2018 September 16 at 10:18:47.891 (The CHIME/FRB Collaboration et al. 2020). Taking the frequency-dependent arrival time of the signal into account, a slightly smaller time gap of 11.69 minutes can be considered by using a dispersion measure of 349.2 pc cm^{-3} (CHIME/FRB Collaboration et al. 2019b), which would cause a burst to be detected in the optical bands 4.025 s before reaching the center of the CHIME band at 600 MHz, i.e., the reference frequency for the reported burst times.

The precise localization of the FRB made it possible to perform forced point-spread function (PSF) photometry in all the available images, assuming that an optical burst would have indeed a PSF profile. A limit based on forced photometry is more reliable than a limit based on the lack of ZTF "alerts" (Bellm et al. 2019) because alerts are affected by blind detection efficiency, which by definition is ~50% around the limiting magnitude, and because forced photometry allows us to lower the discovery threshold. We used `ForcePhot` (Yao et al. 2019) to perform forced PSF photometry on images processed with the ZTF real-time reduction and image subtraction pipeline at the Infrared Processing & Analysis Center (Masci et al. 2019) using the `ZOGY` algorithm (Zackay et al. 2016). Image subtraction helped us obtain cleaner photometry by removing host galaxy flux and reducing stars crowdedness in the field (Figure 1). Upon nondetection of a source at 3σ level, we considered conservative upper limits calculated by the ZTF pipeline.

Forced photometry on 683 images returned three faint detections (on 2018 July 22 11:00:27, 2018 September 28 07:36:45, and 2018 December 31 02:26:04) and 680 nondetections. The three ~3σ detections were deemed spurious because of imperfect image subtraction across the chip and the shape of the residuals hardly approximating a PSF. In conclusion, no optical burst from FRB 180916.J0158+65 was found in ZTF images. We also inspected the images to check that no sign of saturation (which may result in unreliable photometry) was present and that no cosmic ray (CR) hit the CCD at the FRB location during ZTF exposures, since the charge deposition of a CR could mimic the occurrence of an optical flash. With a hit rate of 2 cm^{-2} minutes^{-1}, we could expect about 21 CRs per 3072 × 3072 pixels quadrant per 30 s frame. We corrected the apparent magnitudes for the Galactic dust extinction along the line of sight using the Schlafly & Finkbeiner (2011) dust maps. FRB 180916.J0158+65 is located at low Galactic decl. ($b = 3.72$), which explains the large extinction of $E(B - V) = 0.87$ (Schlafly & Finkbeiner 2011). We note that a lower extinction of $E(B - V) = 0.68$ is obtained using the 3D dust map based on Gaia, Pan-STARRS 1, and 2MASS (Green et al. 2019), so our results obtained using the Schlafly & Finkbeiner (2011) extinction are conservative. The distribution of the 3σ upper limits that we obtained is shown in Figure 3.

3. Statistical Analysis

The objective of the proposed method is to yield statistically robust constraints, under a few assumptions, despite the fact that all detected repetitions of FRB 180916.J0158+65 occurred outside ZTF exposures. In particular, we assume that every FRB is accompanied by a short-duration (≪30 s) optical flash with fluence η times the FRB fluence, then we calculate the limiting probability $\widetilde{P}(\eta)$ as given by ZTF nondetection of

---

[8] All times in this work are expressed in UTC. The full observation log can be found at https://www.astro.caltech.edu/~ia/log_frb_ztf.csv.

Table 1
Limits from ZTF Photometry

Images	Filter	Exptime (s)	Mag (AB)	Mag Corrected (AB)	Seeing	F_{50} (Jy ms)	F_{90} (Jy ms)	F_{95} (Jy ms)	η_{50}	η_{90}	η_{95}
227	g	6810	20.72	17.39	all	12.11	31.17	39.97	1.2	3.1	4.0
173	g	5190	20.88	17.56	$<3''$	10.55	27.87	37.488	1.1	2.8	3.7
456	r	13680	20.22	17.92	all	8.02	201.11	307.12	0.8	20.1	30.7
363	r	10890	20.41	18.11	$<3''$	7.33	58.49	110.90	0.7	5.8	11.1
683	g + r	20490	⋯	⋯	all	9.92	133.78	246.26	1.0	13.4	24.6
536	g + r	16080	⋯	⋯	$<3''$	8.25	42.06	96.99	0.8	4.2	9.7

Note. The first five columns indicate the number of 30 s images analyzed, the filter, the total exposure time, and median limiting magnitude (50% confidence) before and after Galactic extinction correction (Schlafly & Finkbeiner 2011). The quantities are calculated using images taken under all seeing conditions and using only those with seeing $<3''$. Then we report the fluence limit at 50%, 90%, and 95% confidence. Finally, we indicate the ratio between optical and radio fluence assuming an FRB fluence $\mathcal{F}_{frb} = 10$ Jy ms.
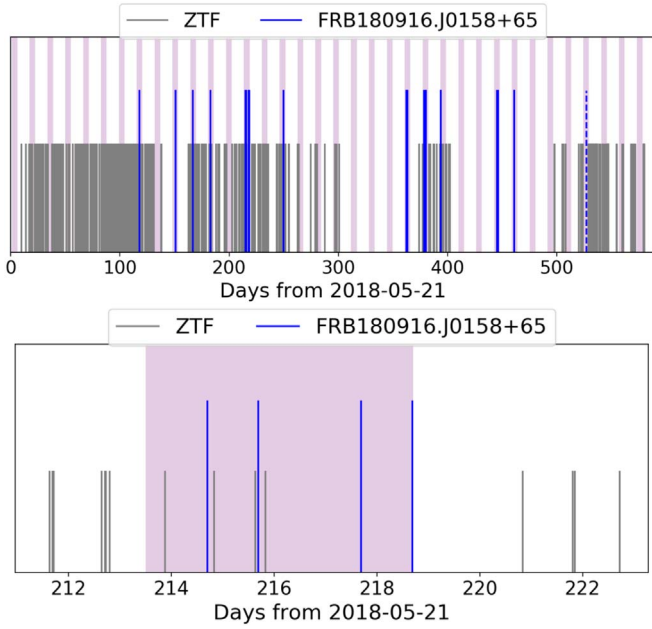
Figure 2. Top: ZTF observations (gray lines) and FRB 180916.J0158+65 detections (blue lines; CHIME/FRB Collaboration et al. 2019b; Marcote et al. 2020; The CHIME/FRB Collaboration et al. 2020). Purple bands indicate regions of high FRB activity, determined using a period of 16.35 days and a time window of 2 × 2.6 days around the estimated activity peak (The CHIME/FRB Collaboration et al. 2020). Dotted lines (unresolved) indicate two FRBs detected on 2019 October 30, after a CHIME instrument upgrade. Bottom: same as the top panel, zoomed in a region of the plot where four bursts were detected, two of which were minutes to hours from ZTF observations.

(The data used to create this figure are available.)

Figure 3. Top: distribution of 3σ upper limits (apparent magnitude in AB system) on 683 ZTF images. Bottom: the same distribution is shown after correcting for Galactic extinction along the line of sight using the Schlafly & Finkbeiner (2011) dust maps.

optical flashes for each η. Radio (FRB) fluence is denoted as $\mathcal{F}$, so the corresponding optical fluence is $F = \eta\mathcal{F}$. The results obtained in this section are agnostic to any assumption of periodic modulation; hence, they are insensitive to possible period aliasing. The detailed procedure is as follows.

We start from the cumulative fluence distribution $N_{frb}(\geqslant\mathcal{F})$ of the CHIME bursts as shown in the Extended Data Figure 3 of The CHIME/FRB Collaboration et al. (2020). A fluence threshold $\mathcal{F}$ is chosen such that there are N_{frb} detections above it. The goal is to construct a statistical model that reproduces the N_{frb} CHIME bursts while determining the number of accompanying optical flashes captured by our ZTF images at the same time. We assume that the time intervals δ between adjacent bursts (above a certain fluence) follows the Weibull
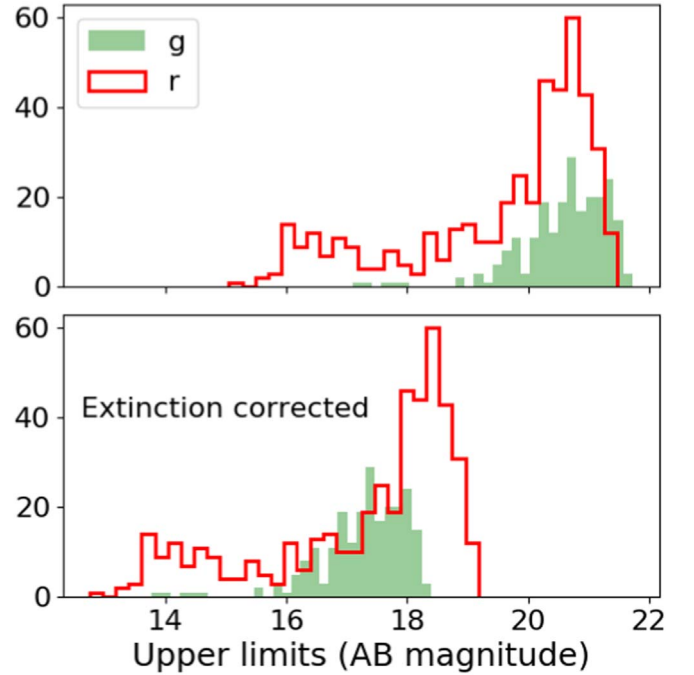
distribution, which has been used to model the first repeater FRB 121102 (Oppermann et al. 2018) and the whole CHIME repeater population (Lu et al. 2020). The cumulative distribution of wait time δ is given by

$$P(<\delta) = 1 - \exp\left[-(r\delta\,\Gamma(1 + 1/k)^k\right], \qquad (1)$$

where k is the Weibull clustering parameter ($k < 1$ describes that small intervals are favored compared to the Poissonian, $k = 1$, case), $r = \langle\delta\rangle^{-1}$ is the mean repeating rate, and $\Gamma(x)$ is the gamma function. Note that $k \simeq 1/3$ is favored by analysis of the first repeater FRB 121102 (Oppermann et al. 2018; Oostrum et al. 2020).

Our $t = 0$ corresponds to 2018 May 31 11:19:32 when the first ZTF exposure starts, and then the starting time of the lth ZTF observation is denoted t_l^{ztf} (with $t_0^{ztf} = 0$ by definition and $l = 0, 1, ..., 682$). We randomly draw successive time intervals δ_i such that the nth FRB and optical flash occur at time $t_n = t_0 + \sum_{i=0}^{n} \delta_i$, where t_0 is a negative random number

between $-30/r$ and $-10/r$ such that the first ZTF exposure time ($t = 0$) is far from the start of burst series ($t = t_0$). CHIME exposures start on 2018 August 28 (The CHIME/FRB Collaboration et al. 2020) and occur regularly on a (sidereal) daily basis, so we take the starting time for each CHIME observation to be $t_m^{chime} = (90.5 + \xi m)$ days (the precise value of t_0^{chime} is unimportant), where $\xi \equiv 23.9344696/24$ is the scale factor for the length of a sidereal day. With three time series $\{t_n\}$ (FRB occurrence, randomly generated), $\{t_l^{ztf}\}$ (start time of ZTF exposures, fixed), and $\{t_m^{chime}\}$ (start time of CHIME daily on-sky exposures, fixed), the nth burst is recorded as detectable by ZTF (or CHIME) if $t_l^{ztf} < t_n < t_l^{ztf} + \Delta^{ztf}$ (or $t_m^{chime} < t_n < t_m^{chime} + \Delta^{chime}$), where $\Delta^{ztf} = 30$ s and $\Delta^{chime} = 12$ minutes are the durations of each ZTF and CHIME daily exposures, respectively. We use the CHIME data up to 2019 September 30, so the index for CHIME is $m = 0, 1, \ldots, 398$. During this time, observations were sometimes interrupted by testing, so we randomly take away a fraction $f_{off} = 0.16$ of the daily exposures, meaning that no detection is recorded for the off-line day even if $t_m^{chime} < t_n < t_m^{chime} + \Delta^{chime}$. This reduction gives a total exposure time of 2.7 days or 64 hr, consistent with the estimate by The CHIME/FRB Collaboration et al. (2020). We exclude two CHIME bursts detected on 2019 October 30 (dashed blue lines in Figure 2) in our repeating rate estimation, because they are detected after a major pipeline upgrade.

With the above procedure, for each set of parameters $\{r, k\}$ (mean repeating rate and temporal clustering), we carry out $N_{cases} = 1000$ random cases and determine the detected number of bursts by CHIME (N_{chime}) and the number of optical flashes within the ZTF coverage (N_{ztf}). The likelihood that this set of parameters reproduces the CHIME data is given by $L = \sum (N_{chime} = N_{frb})/N_{cases}$, where $\sum (N_{chime} = N_{frb})$ is the number of cases that match the number of observed bursts above a certain fluence $\mathcal{F}$. We have tested that N_{cases} is sufficiently large to yield a stable likelihood whose random fluctuation is negligible compared to other uncertainties of our problem. More realistically, the likelihood should also include the goodness of fit between the simulated and observed distributions of time intervals between adjacent bursts, which will constrain the Weibull parameter k (Oppermann et al. 2018; Oostrum et al. 2020). Instead, we take a number of different fixed $k \in (1/4, 1/2)$ and treat the resulting difference as the systematic error of our method. This is motivated by the fact that the expected number of ZTF detections mainly depends on the mean repeating rate r. For the same reason, the 16 day periodicity of FRB 180916.J0158+65 raises the mean repeating rate within the ± 2.6 day (the exact numbers are unimportant) active window by a factor of 16/5.2 in *both* the CHIME and ZTF observing runs coincident with the active windows, so our method is insensitive to the periodicity. Then, for each k, we use the following Markov Chain Monte Carlo (MCMC) method to constrain $\log r[\text{day}^{-1}]$ and simultaneously determine the probability $P(N_{ztf} \geqslant 1)$. Hereafter the mean repeating rate r is in units of day^{-1}.

The initial value is taken to be $\log \bar{r}$ and we assume a flat prior of $\log r \in (\log \bar{r} - 1, \log \bar{r} + 1)$, where $\bar{r} = N_{frb}/2.7$ days is the mean expectation. We record the probability of at least one optical flash occurring within ZTF exposures $P_i(N_{ztf,i} \geqslant 1)$ for each accepted sample of $\log r_i$. Finally, for an assumed fluence ratio η between optical flashes and FRBs, the probability that ZTF captured at least one optical
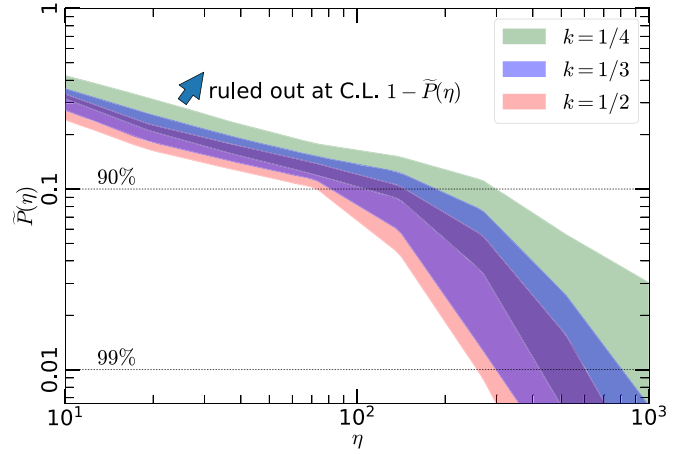

Figure 4. Limits on the optical-to-radio fluence ratio $\eta = F/\mathcal{F}$ from nondetection of optical flashes with ZTF. The probability that η is allowed is denoted as $\widetilde{P}(\eta)$, so each η is ruled out at confidence level (C.L.) of $1 - \widetilde{P}(\eta)$. The three colored bands are for different $k = 1/4$ (green), 1/3 (blue, our fiducial case), 1/2 (red), with decreasing $\widetilde{P}(\eta)$. The upper and lower bounds for each band are for $\gamma = 1.8$ and 2.4, respectively. Generally, we rule out $\eta \simeq 200$, or $E_{opt} \simeq 3 \times 10^{46}$ erg associated with an FRB with $\mathcal{F} = 10$ Jy ms, at 90% confidence level.

flashes brighter than $\eta\mathcal{F}$ is given by

$$P_d(\mathcal{F}, \eta) = \sum_i P(N_{ztf,i} \geqslant 1)/N_{samp}, \qquad (2)$$

where N_{samp} is the total number of accepted MCMC samples (convergence is achieved for $N_{samp} \gtrsim 3 \times 10^5$). The above probability is a decreasing function of the FRB fluence cut $\mathcal{F}$, because $N_{frb}(\geqslant \mathcal{F})$ and hence the mean repeating rate r decrease with $\mathcal{F}$.

On the other hand, our nondetection in all 683 ZTF images rule out any flash brighter than $\eta\mathcal{F}$ (beyond 3σ) at probability $P_{nd}(\eta\mathcal{F})$. Thus, we are able to rule out the particular fluence ratio η with survival probability $\widetilde{P} = 1 - P_d(\mathcal{F}, \eta)P_{nd}(\eta\mathcal{F})$. For a given η, we try a number of different fluence cuts $\mathcal{F} \in (6, 20)$ Jy ms and the corresponding observed $N_{frb}(\geqslant \mathcal{F})$, and the best constrained case gives the lowest survival probability $\widetilde{P}(\eta)$. Below the CHIME completeness threshold $\mathcal{F} \simeq 6$ Jy ms, instead of taking the detected number, we use power-law $N_{frb}(\geqslant \mathcal{F}) \propto \mathcal{F}^{1-\gamma}$ extrapolation. Steeper power law (larger γ) will give more FRBs at low fluences and hence stronger constraints on η. We show the results for $\gamma = 1.8$, as motivated by the study of the CHIME repeating sample (Lu et al. 2020), and for $\gamma = 2.4$, as indicated by the apparent fluence distribution of FRB 180916.J0158+65 (The CHIME/ FRB Collaboration et al. 2020).

4. Results

The analysis described in Section 3 provides a framework to robustly combine ZTF measurements and CHIME detections of a repeating FRB, even if the detected radio bursts were not coincident with ZTF observations of the source. As shown in Figure 4, we are able to constrain $\eta \lesssim 200$ at 90% confidence level, corresponding to a limit on the energy of $E_{opt} \lesssim 3 \times 10^{46}$ erg for an optical counterpart associated with a $\mathcal{F} = 10$ Jy ms FRB.

The results can be understood as follows. The expectation value of the repeating rate above threshold $F_{th} = 5$ Jy ms is about 1 hr^{-1} within the ± 2.6 day active windows (The

CHIME/FRB Collaboration et al. 2020). If we simply *assume* a rate of $r (>5 \, \mathrm{Jy \, ms}) = 1 \, \mathrm{hr}^{-1}$, then on average 1.2 ± 1.1 optical flashes are expected to occur in our 147 ZTF images acquired within the active windows. The ZTF limits in those time frames yield $F_{95} \simeq 30 \, \mathrm{Jy \, ms}$ (95% confidence), which means that we can rule out $\eta = F_{95}/\mathcal{F}_{\mathrm{th}} \simeq 3$ at 95% confidence. However, the repeating rate of $r (>5 \, \mathrm{Jy \, ms})$ is highly uncertain. Our method in Section 3 combines the probability distributions of both the repeating rate and the ZTF limiting fluence and hence gives a robust statistical constraint on η that is a factor of $\sim$100 less stringent than the above simple expectation.

5. Discussion

Optical observations of FRB 180916.J0158+65 with high cadence were performed by Zampieri et al. (2020) using the fast optical photon counter IFI+IQUEYE (Naletto et al. 2009) mounted on the 1.2 m Galileo telescope. Although no FRB was detected during their observations, Zampieri et al. (2020) placed an upper limit on the optical fluence of $F \lesssim 0.151$ Jy ms,[9] which is more constraining than ZTF results thanks to the significantly shorter exposure time. Zampieri et al. (2020) also obtained results (see footnote 9) comparable with ZTF using the 67/92 Schmidt telescope near Asiago, Italy.

Hardy et al. (2017) place constraints on the optical fluence of FRB 121102 using 70 ms exposures coincident with radio observations, obtaining $E_{\mathrm{opt}} \lesssim 10^{43}$ erg (or equivalent fluence ratio $\eta \lesssim 0.02$ for the brightest FRB). Similarly, MAGIC Collaboration et al. (2018) observed FRB 121102 using the Major Atmospheric Gamma Imaging Cerenkov simultaneously with Arecibo. Along with five radio bursts, they detected no optical U-band bursts with fluence $>9 \times 10^{-3}$ Jy ms (see footnote 9) at 1 ms exposure time bins, although one optical burst was found 4 s before an FRB, with 1.5% random association probability. We note that there was no explicit mention to Galactic extinction correction in previous work discussed in this section. FRB 121102 is also located close to the Galactic plane ($b = -0.22$ deg), where the extinction is significant. The effect should be smaller for Hardy et al. (2017) than for ZTF g- and r-band observations, thanks to their redder $i' + z'$ broadband filter. The excellent limit placed by MAGIC Collaboration et al. (2018) may suffer a larger correction for the U band, which should be taken into account in multiwavelength FRB modeling.

Our current 90% limit of $\eta \simeq 200$ corresponds to an optical-to-radio *energy* ratio of $\eta \nu_{\mathrm{opt}}/\nu_{\mathrm{frb}} \sim 10^8$, which is at least two to three orders of magnitude above the predictions of the synchrotron maser model based on magnetar flares (assuming pair-dominated upstream plasma; Beloborodov 2019; Metzger et al. 2019). However, our constraint can be significantly improved with shorter per-image exposure time and longer total integration time in future observations. We also note that, assuming the same observing sequence, ZTF observations at high Galactic latitude (with negligible dust extinction) would yield an order of magnitude deeper constraints on the fluence.

6. Summary and Future Prospects

In this work, we placed constraints on the optical fluence of FRB 180916.J0158+65 using 683 images serendipitously

---

[9] Galactic extinction correction is not addressed.

acquired with ZTF. The statistical analysis presented in Section 3 combined disjointed ZTF exposures and CHIME detections into a robust upper limit on optical-to-radio fluence ratio $\eta \lesssim 200$ (90% confidence) and on the emitted energy in the optical $E_{\mathrm{opt}} \lesssim 3 \times 10^{46}$ erg for a 10 Jy ms FRB.

This work further demonstrated that possible optical counterparts to FRBs can be constrained with large field-of-view optical surveys such as ZTF, TESS (see also the search for optical counterparts to FRB 181228 by Tingay & Yang 2019), and soon the Legacy Survey of Space and Time (LSST) at Vera Rubin Observatory. As Table 1 suggests, ZTF has the potential of placing deeper constraints when bright ($\mathcal{F} > 10 \, \mathrm{Jy \, ms}$) FRBs are simultaneously observed, especially at high Galactic latitudes. New high-cadence instruments can also play an important role in FRB counterpart detection with subsecond observations. These include drift scan imaging experiments (Tingay 2020), the wide-field Tomo-e Gozen instrument (Sako et al. 2016; Richmond et al. 2020), or the Weizmann Fast Astronomical Survey Telescope (WFAST; Nir et al. 2017) based on complementary metal-oxide-semiconductor (CMOS) technology, or the Ultra-Fast Astronomy (UFA; Li et al. 2019) observatory that will observe variable sources at millisecond to nanosecond timescales using two single-photon-resolution fast-response detectors.

This work also showed that nearby, highly active FRBs such as FRB 180916.J0158+65 present us with ground for statistical estimates of optical fluence limits even without simultaneous optical+radio observations. Dedicated high-cadence experiments may have higher chances of detecting optical flashes from FRBs, for example using the Caltech HIgh-speed Multi-color camERA (CHIMERA; Harding et al. 2016) mounted at the prime focus of the large 200 inch Hale Telescope at Palomar Observatory. CHIMERA could yield constraints up to 100 times deeper than any existing optical observation to date. On the other hand, Chen et al. (2020) suggest a different method to quantify the presence of FRB counterparts in the existing data sets of large, continuous multiwavelength and multimessenger surveys. In conclusion, the near future offers a plenty of opportunities to further investigate optical counterparts to FRBs.

Appendix
Optical Flash Detectability with ZTF

In this appendix, we describe the response of ZTF CCDs if bright optical flashes are observed. The *creation* of electron hole pairs when photons are absorbed is effectively instantaneous and is linear, i.e., the absorption probability is not affected by the photon flux since the density of valence band electrons available to be promoted to the conduction band is very high compared to the photon flux. The *collection* of photogenerated charge is lossless and thus linear only if clock voltages are set to prevent charge from interacting with traps at the surface. For present clock settings in ZTF, this is not the case during exposure since clocks are positively biased to minimize lateral charge diffusion at the expense of linearity beyond saturation. However, we visually checked all the processed images and none showed signatures of saturation.

A possible effect of very high flux is electrostatic repulsion of photogenerated charges. An illustrative example of this effect occurs when (rare) α particles generated by radioactive decay of uranium or thorium occur in the bulk silicon (Aguilar-Arevalo et al. 2015). Having energies ~ 4 MeV, these α particles deposit $\gtrsim 4$ million electrons, since the bandgap in silicon is 1.14 eV. These α particle events cover a circular area whose size depends on the thickness of the field-free region. The effect is well documented in thick fully depleted CCDs and typically spans 5–6 pixels (Aguilar-Arevalo et al. 2015).

Data for the equivalent electrostatic repulsion prior to charge collection is scarce in the standard CCDs used in ZTF. These have a field-free region near the back surface that is estimated to vary from 10 to 20 μm in a radial pattern, based on overall thickness implied by surface metrology and confirmed by fringing patterns from night sky lines. Once the charge diffuses toward the potential wells, the PSF depends on signal in well-known ways: brighter–fatter effect (Guyonnet et al. 2015), charge blooming, tails due to charge transfer inefficiency, and signal nonlinearity. These effects are not expected to significantly affect the limits calculated in this work.

ORCID iDs

Igor Andreoni ● https://orcid.org/0000-0002-8977-1498
Wenbin Lu ● https://orcid.org/0000-0002-1568-7461
Frank J. Masci ● https://orcid.org/0000-0002-8532-9395
Eric C. Bellm ● https://orcid.org/0000-0001-8018-5348
Matthew J. Graham ● https://orcid.org/0000-0002-3168-0139
David L. Kaplan ● https://orcid.org/0000-0001-6295-2881
Mansi M. Kasliwal ● https://orcid.org/0000-0002-5619-4938
Thomas Kupfer ● https://orcid.org/0000-0002-6540-1484
Russ R. Laher ● https://orcid.org/0000-0003-2451-5482
Ashish A. Mahabal ● https://orcid.org/0000-0003-2242-0244
Thomas A. Prince ● https://orcid.org/0000-0002-8850-3627
Reed Riddle ● https://orcid.org/0000-0002-0387-370X
Yuhan Yao ● https://orcid.org/0000-0001-6747-8509

References

Aguilar-Arevalo, A., Amidei, D., Bertou, X., et al. 2015, JInst, 10, P08014
Bellm, E. C., Kulkarni, S. R., Graham, M. J., et al. 2019, PASP, 131, 018002
Beloborodov, A. M. 2019, arXiv:1908.07743
Bhandari, S., Keane, E. F., Barr, E. D., et al. 2018, MNRAS, 475, 1427
Bochenek, C., Kulkarni, S., Ravi, V., et al. 2020, ATel, 13684, 1
Casentini, C., Verrecchia, F., Tavani, M., et al. 2020, ApJL, 890, L32
Chen, G., Ravi, V., & Lu, W. 2020, arXiv:2004.10787
CHIME/FRB Collaboration, Amiri, M., Bandura, K., et al. 2018, ApJ, 863, 48
CHIME/FRB Collaboration, Amiri, M., Bandura, K., et al. 2019a, Natur, 566, 235
CHIME/FRB Collaboration, Andersen, B. C., Bandura, K., et al. 2019b, ApJL, 885, L24
DeLaunay, J. J., Fox, D. B., Murase, K., et al. 2016, ApJL, 832, L1
Farah, W., Flynn, C., Bailes, M., et al. 2018, MNRAS, 478, 1209
Fonseca, E., Andersen, B. C., Bhardwaj, M., et al. 2020, ApJL, 891, L6
Graham, M., Kulkarni, S. R., Bellm, E. C., et al. 2019, PASP, 131, 078001
Green, G. M., Schlafly, E., Zucker, C., Speagle, J. S., & Finkbeiner, D. 2019, ApJ, 887, 93
Guyonnet, A., Astier, P., Antilogus, P., Regnault, N., & Doherty, P. 2015, A&A, 575, A41
Harding, L. K., Hallinan, G., Milburn, J., et al. 2016, MNRAS, 457, 3036
Hardy, L. K., Dhillon, V. S., Spitler, L. G., et al. 2017, MNRAS, 472, 2800
Kocz, J., Ravi, V., Catha, M., et al. 2019, MNRAS, 489, 919
Kumar, P., Shannon, R. M., Osłowski, S., et al. 2019, ApJL, 887, L30
Li, S., Smoot, G. F., Grossan, B., et al. 2019, Proc. SPIE, 11341, 113411Y
Lu, W., Piro, A. L., & Waxman, E. 2020, arXiv:2003.12581
MAGIC Collaboration, Acciari, V. A., Ansoldi, S., et al. 2018, MNRAS, 481, 2479
Marcote, B., Nimmo, K., Hessels, J. W. T., et al. 2020, Natur, 577, 190
Martone, R., Guidorzi, C., Margutti, R., et al. 2019, A&A, 631, A62
Masci, F. J., Laher, R. R., Rusholme, B., et al. 2019, PASP, 131, 018003
Metzger, B. D., Margalit, B., & Sironi, L. 2019, MNRAS, 485, 4091
Naletto, G., Barbieri, C., Occhipinti, T., et al. 2009, A&A, 508, 531
Nir, G., Ofek, E. O., Ben-Ami, S., et al. 2017, AAS Meeting, 229, 155.06
Oostrum, L. C., Maan, Y., van Leeuwen, J., et al. 2020, A&A, 635, A61
Oppermann, N., Yu, H.-R., & Pen, U.-L. 2018, MNRAS, 475, 5109
Panessa, F., Savchenko, V., Ferrigno, C., Bazzano, A., & Ubertini, P. 2020, ATel, 13466, 1
Petroff, E., Bailes, M., Barr, E. D., et al. 2015, MNRAS, 447, 246
Pilia, M., Burgay, M., Possenti, A., et al. 2020, arXiv:2003.12748
Ravi, V. 2019, NatAs, 3, 928
Ravi, V., Catha, M., D'Addario, L., et al. 2019, Natur, 572, 352
Richmond, M. W., Tanaka, M., Morokuma, T., et al. 2020, PASJ, 72, 3
Sako, S., Osawa, R., Takahashi, H., et al. 2016, Proc. SPIE, 9908, 99083P
Schlafly, E. F., & Finkbeiner, D. P. 2011, ApJ, 737, 103
Scholz, P., Bogdanov, S., Hessels, J. W. T., et al. 2017, ApJ, 846, 80
Scholz, P., Cook, A., Cruces, M., et al. 2020, arXiv:2004.06082
Scholz, P., Spitler, L. G., Hessels, J. W. T., et al. 2016, ApJ, 833, 177
Shannon, R. M., Macquart, J. P., Bannister, K. W., et al. 2018, Natur, 562, 386
Shannon, R. M., & Ravi, V. 2017, ApJL, 837, L22
Spitler, L. G., Scholz, P., Hessels, J. W. T., et al. 2016, Natur, 531, 202
Tavani, M., Verrecchia, F., Casentini, C., et al. 2020, ApJL, 893, L42
The CHIME/FRB Collaboration, Amiri, M., Andersen, B. C., et al. 2020, arXiv:2001.10275
Tingay, S. 2020, PASA, 37, e015
Tingay, S. J., & Yang, Y.-P. 2019, ApJ, 881, 30
Yao, Y., Miller, A. A., Kulkarni, S. R., et al. 2019, ApJ, 886, 152
Zackay, B., Ofek, E. O., & Gal-Yam, A. 2016, ApJ, 830, 27
Zampieri, L., Burtovoi, A., Fiori, M., et al. 2020, ATel, 13493, 1